

## EXPERIMENTAL BEHAVIOUR OF FLEXURE-CRITICAL STEEL- PLATE COMPOSITE STRUCTURAL WALLS

Siamak Epackachi<sup>1</sup>, Andrew S. Whittaker<sup>2</sup>, Amit Varma<sup>3</sup>

<sup>1</sup> Postdoctoral Research Associate, Dept. of Civil, Structural and Environmental Engineering, University at Buffalo, NY 14260 (siamakep@buffalo.edu)

<sup>2</sup> Professor and Chair; Director, MCEER; Dept. of Civil, Structural and Environmental Engineering, University at Buffalo, Buffalo, NY 14260 (awhittak@buffalo.edu)

<sup>3</sup> Professor, School of Civil Engineering, Purdue University, IN 47907 (ahvarma@purdue.edu)

### ABSTRACT

An experimental program on steel-plate concrete (SC) composite shear walls was executed in the NEES laboratory at the University at Buffalo. Four large-size specimens were tested under displacement-controlled cyclic loading. The design variables considered in the testing program included wall thickness, reinforcement ratio, and faceplate slenderness ratio. The aspect ratio (height-to-length) of the four walls was 1.0. Each SC wall was installed on top of a re-usable foundation block. A bolted baseplate to RC foundation connection was used for all four walls. Results of the four SC wall experiments are presented, including damage to the SC walls at different drift ratios, the cyclic force-displacement relationships, energy dissipation and equivalent viscous damping ratios, and the contributions of shear, flexure, and base rotation to the total lateral displacement. These data, and that now available at NEESHUB, can be used to develop analytical and numerical models for SC walls.

### INTRODUCTION

SC walls consisting of steel faceplates, infill concrete, and connectors used to anchor the steel faceplates together and to the infill concrete, have potential advantages over conventional reinforced concrete and steel plate shear walls in terms of constructability and seismic performance. SC panels enable modular construction leading to potential time and cost savings over conventional reinforced concrete walls. Double skin SC wall shells can be fabricated offsite, assembled on site, and filled on-site with concrete to create monolithic structure. The use of steel faceplates eliminates the need for on-site formwork, and the faceplates serve as primary reinforcement.

The number of applications to date of SC walls is limited. Most proposals for SC wall construction have involved two steel faceplates with infill concrete ( e.g., Fukumuto et al. [8], Wright et al. [12-14], Tomlinson et al. [9], and Bowerman et al. [1]). The use of SC wall construction in nuclear power plants has been studied for nearly 20 years, with an emphasis on elastic response in design basis shaking. Safety-related nuclear applications have involved steel faceplates and infill (unreinforced) concrete, where the faceplates provide formwork and reinforcement, and the SC walls provide both gravity and earthquake resistance, without the introduction of internal steel framing for gravity-load resistance. Application of SC walls to containment internal structures and shield buildings in nuclear power plants has begun in the United States and China, with US applications based substantially on the work of Varma and his co-workers at Purdue University (e.g., Varma et al.[10, 11] and Zhang et al. [15]). SC walls have not been used for earthquake-resistant building construction, in part because there is little data on the seismic performance of these walls at deformation levels expected in buildings subjected to maximum earthquake shaking.

To date, design of SC walls (for nuclear applications) has been based in part on proprietary test data and the limited data available in the literature. Most of the experiments were conducted at small scales and focused on the essentially elastic range of response. The small-scale tests cannot represent reality well

because construction materials and conditions are generally very different from those used for field applications.

This paper assesses the seismic performance of flexure-critical SC walls through testing of four large-size rectangular steel-plate concrete (SC) composite shear walls under displacement-controlled cyclic loading. The SC wall piers consisted of two steel faceplates, infill concrete, headed steel studs anchoring the faceplates to the infill, and tie rods connecting the two faceplates through the infill. Only loading in the plane of the wall is considered. The following sections of the paper describe the experimental program, present key experimental results. The numerical models developed for the finite element analysis of SC walls and the analytical model developed for the monotonic analysis of fixed-base SC wall piers are described elsewhere (e.g., Epackachi et al. [6, 7]). The data presented here and that now available at NEESHUB [4] can be used to develop other numerical and analytical models of SC walls.

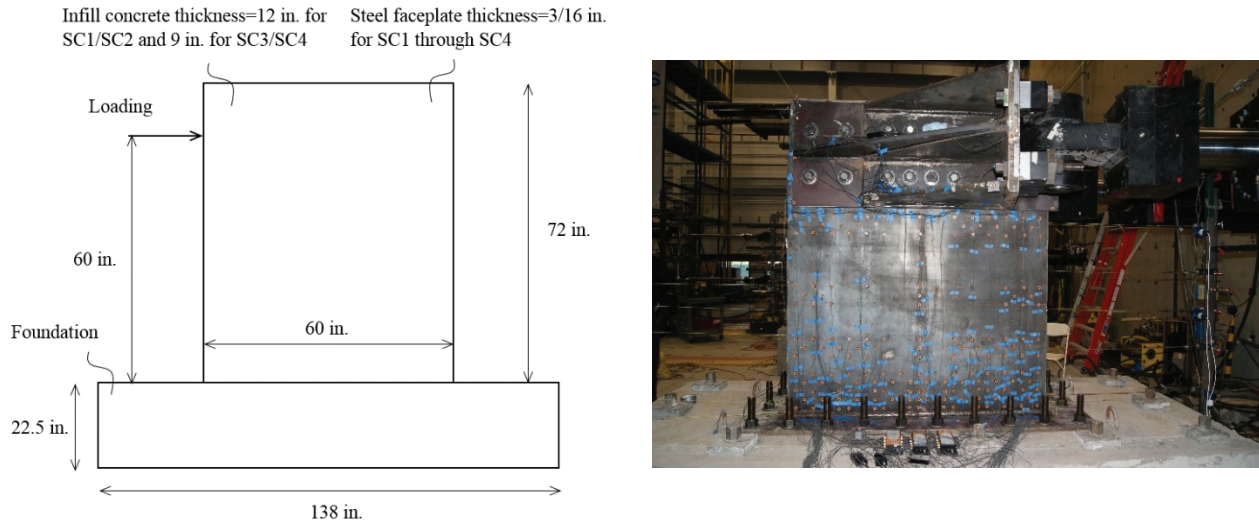
## EXPERIMENTAL PROGRAM

### *Description of the Test Specimens*

Four large-scale rectangular SC wall specimens (SC1 through SC4) with an aspect ratio of 1.0 were subjected to displacement-controlled cyclic loading in the NEES laboratory at the University at Buffalo. The height and the length of the wall specimens were 72 in. and 60 in., respectively. The distance between the top of the baseplate and the center line of the loading plates was 60 in. The wall thickness was 12 in. for SC1 and SC2 and 9 in. for SC3 and SC4. Two 0.18 in.-thick steel faceplates were used in each wall. The diameter of the studs and tie rods was 0.375 in. for all walls. Studs and tie rods were used in SC1 and SC3 but only tie rods were used in SC2 and SC4, in part to permit the removal of the faceplates from SC2 and SC4, to allow examination of the damage to the infill concrete. The studs were spaced 4 in. and 4.5 in. on center in SC1 and SC3, respectively. Tie rods were spaced 12 in., 6 in., 9 in., and 4.5 in. on center in SC1 through SC4, respectively. A schematic of the walls and a photograph of SC1 are presented in Figure 1.

The design variables considered in the experiments were wall thickness of 9 in. and 12 in., reinforcement ratio of 3.1% and 4.2%, slenderness ratio ranging from 21 to 32, where reinforcement ratio is defined as the ratio of the cross-sectional area of the faceplates divided by the total cross-sectional area of the SC wall and the slenderness ratio is defined as the ratio of the greatest spacing of the connectors (studs or tie rods) to the steel faceplate thickness. Pre-test cross-sectional and finite element analyses of the four SC walls indicated that these walls would be flexure-critical [5].

A post-tensioned bolted connection was used to anchor the SC specimens to a foundation block. The connection consisted of an 1-in. thick steel plate embedded in the foundation block, an 1-in. thick baseplate attached to the steel faceplates, 22 number 1.25-in. diameter threaded bars securing the baseplate to the foundation block, headed studs attached to the baseplate, shear lugs attached to the steel plate embedded in the foundation block, and a steel anchorage securing the threaded bars to the foundation block. Post-tensioned Dwyidag bars were used to anchor the foundation block to the strong floor. The baseplate, threaded bars, and the Dwyidag bars were sized to remain elastic, with a margin, under the maximum predicted shear force of 350 kips. The details of test setup, loading protocol, and instrumentation of the specimens are described in [3, 5].



## Experimental results

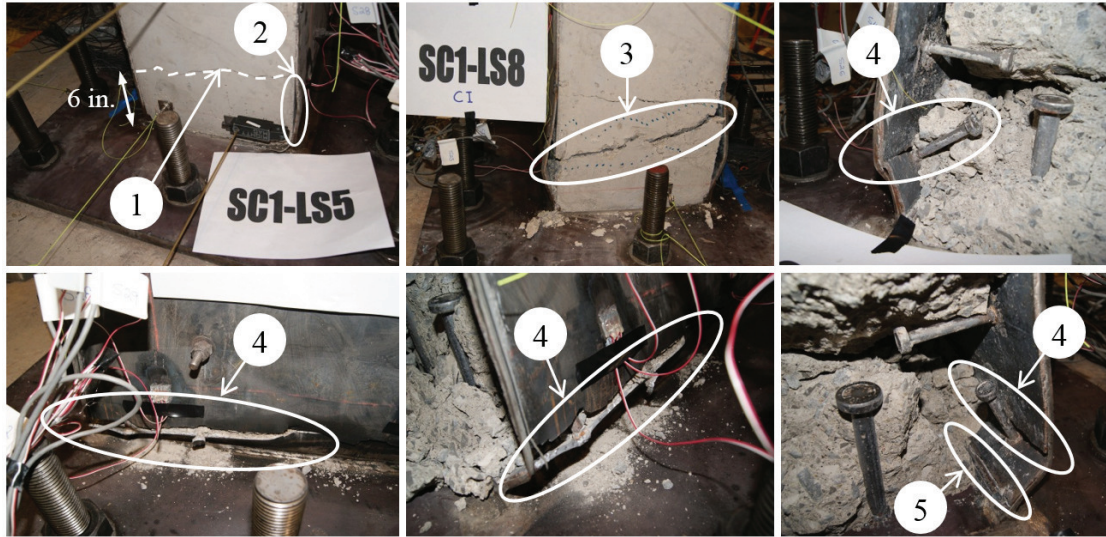
### *Damage to SC Walls*

Figure 2 presents the damage to SC1 through SC4 at different drift ratios. In Figure 2, LS denotes the load step, and CI and CII represent the first and second cycles in each load step, respectively. The sequence of the damage to the SC walls is presented in Table 1. Tearing of the steel faceplates initiated immediately above the welded connection of the faceplates to the baseplate in SC2, SC3, and SC4. In SC1, the steel faceplates fractured first at connections to the headed studs. This issue is attributed to the effect of studs and tie rods on the damage to SC walls. The lower corners of the steel faceplates, where the faceplates were expected to buckle, were restrained by headed studs in SC1 and tie rods in the other SC walls (see Figure 3). Headed studs anchor the faceplates to the infill concrete, enable composite action, and delay out-of-plane buckling of the faceplates. Crushed concrete around a stud cannot anchor a stud and local damage around the stud will affect the buckling resistance of the faceplate.

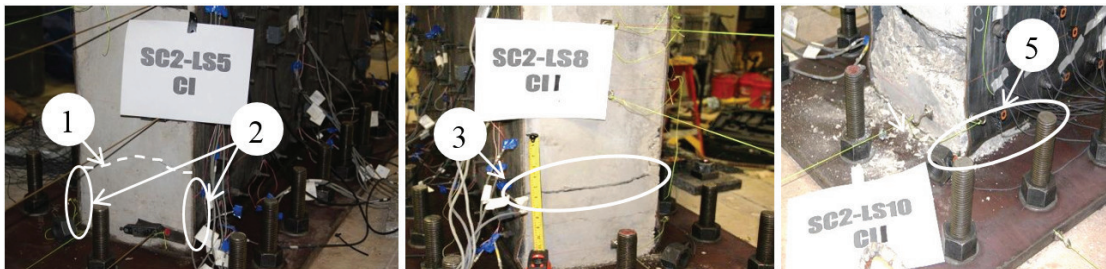
### *Load-displacement Cyclic Response*

The load-displacement relationships for SC1 through SC4 are presented in Figure 4. Points A, B, C, D, E, F, and G in Figure 4 represent the onset of concrete cracking, yielding of the steel faceplates, buckling of the steel faceplates, concrete crushing, fracture of the steel faceplates at their connection to the headed studs, tearing of the steel faceplate above the welded connection of the faceplates to the baseplate, and fracture of tie rods, respectively. The load was calculated by resolving the sum of the forces in the actuator load cells into the plane of the wall. The displacement was measured by a Temposonic displacement transducer attached to the side of the wall at the level of the actuators (60 in. above the base of the wall).

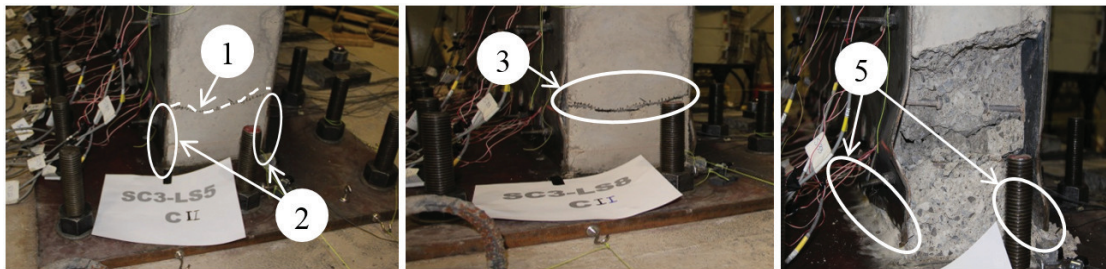
The peak load, observed at a relatively high drift ratio of 1.17+%, were 325 kips and 275 kips for SC1/SC2, and SC3/SC4, respectively. The pinched behavior was attributed to the damage to the infill concrete and steel faceplates, including concrete crushing and tearing of the steel faceplates, and flexibility at the base of the wall. The rates of the post-peak strength and stiffness deterioration were similar in SC2, SC3, and SC4. The rate of strength deterioration in SC1 post-peak-strength was much lower than in the other walls up to point F in SC1 (2.33% drift ratio), where the steel faceplates fractured above their welded connection to the baseplate.



(a) SC1



(b) SC2



(c) SC3



(d) SC4

1. Concrete cracking; 2. Steel faceplate buckling; 3. Concrete crushing; 4. Fracture of the steel faceplate at the level of the stud; 5. Fracture of the steel faceplate above the welded connection; 6. Fracture of a tie rod

Figure 2. Damage to SC walls

Table 1. Sequence of damage to SC walls

Load step	Drift ratio	Specimen	Damage
LS2	0.12%	SC1 through SC4	Concrete cracking at the toes of the wall
LS5	0.47%	SC1 through SC4	Buckling of the steel faceplates
LS8	1.17%	SC1 through SC4	Concrete crushing at toes of the wall
LS9	1.40%	SC3 and SC4	Tearing of the steel faceplates immediately above the welded connection of the faceplates to the baseplate
LS10	1.63%	SC1	Local tearing of the steel faceplates at the connection point to the steel studs
		SC2	Horizontal tearing of the steel faceplates immediately above the welded connection of the faceplates to the baseplate
LS12	2.10%	SC4	Fracture of a tie rod
LS13	2.33%	SC1	Horizontal tearing of the steel faceplates at the level of the steel studs and immediately above the welded connection of the faceplates to the baseplate

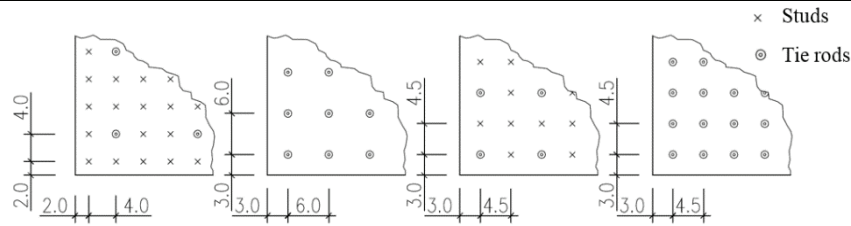


Figure 3. Location of the studs and tie rods attached to the steel faceplates

The onset of yielding of the steel faceplates was determined using the rosette strain gage data and assuming a Von-Mises yield criterion. As seen in Figure 4, yielding of the steel faceplates occurred prior to their buckling for SC1 and SC2. Buckling and yielding of the steel faceplates occurred at the same drift ratio for SC3 and SC4. Concrete crushing occurred at a drift ratio steel corresponding to the peak shear strength for the four SC walls.

The pre-peak-strength response of these flexure-critical SC walls could be approximated by a tri-linear force-displacement relationship to consider three stages of response, namely 1) elastic, 2) cracking of the infill concrete, and 3) buckling of the steel faceplates.

### ***Energy Dissipation and Viscous Damping***

The cumulative energy dissipation in the SC walls is presented in Figure 5. The energy dissipated in each cycle was calculated as the area enclosed by the hysteresis loop in that cycle. The cumulative energy dissipation capacity of the thicker walls, with higher peak loads was expected to be greater than that of the thinner walls. The energy dissipation in SC4 was greater than that in SC2 due to a lower rate of post-peak strength deterioration in SC4 than in SC2.

Equation (1) [2] was used to calculate the equivalent viscous damping,  $\xi_{eq}$ , in the SC walls:

$$\xi_{eq} = \frac{1}{4\pi} \frac{E_D}{E_S} \quad (1)$$

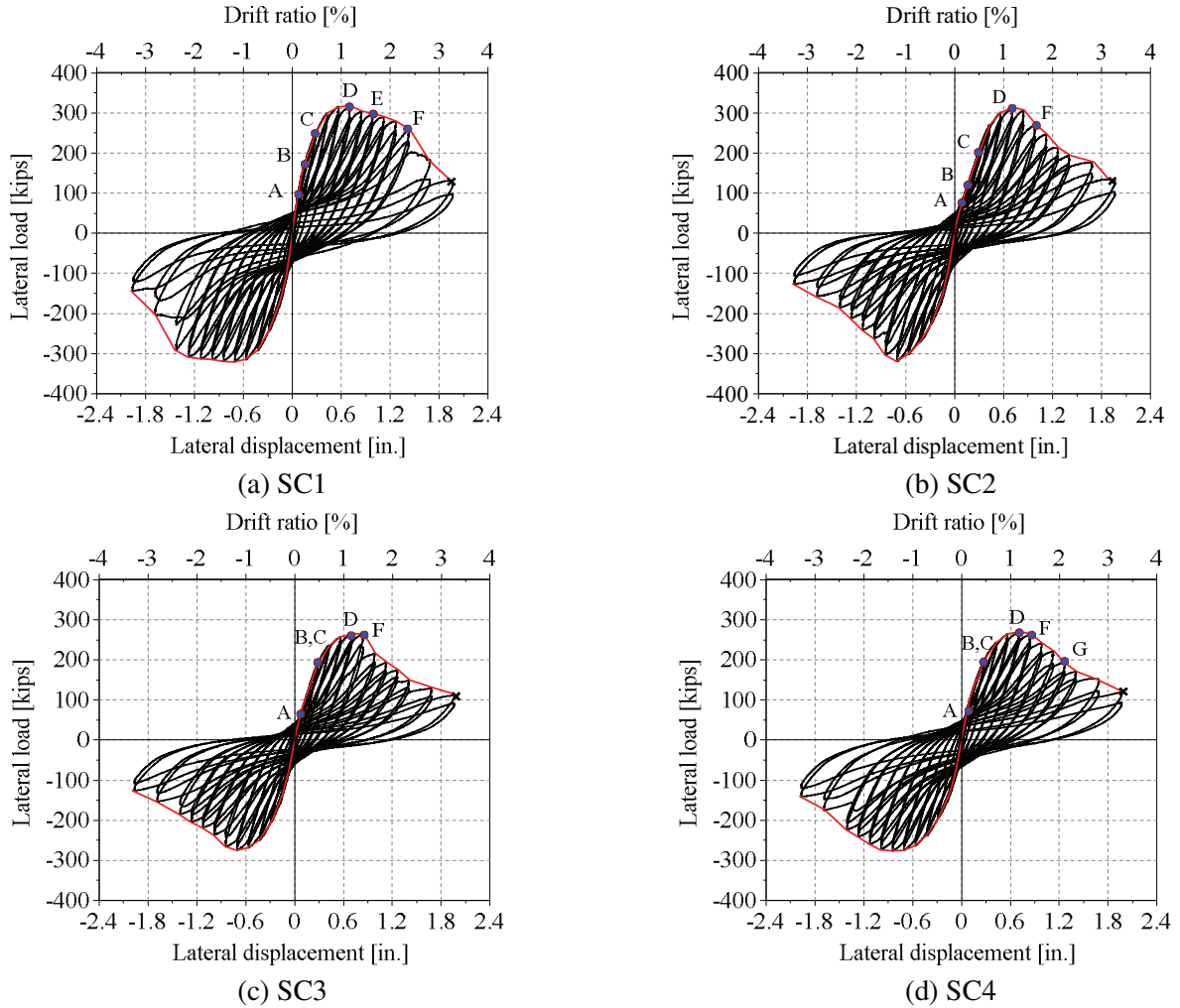


Figure 4. Cyclic force-displacement relationships and backbone curves for the SC walls

Figure 6 presents the equivalent viscous damping ratio calculated from the experimental data for drift ratios up to 3.3%. The vertical dashed red line represents the drift ratio corresponding to peak strength. In the pre-peak-strength region, the equivalent viscous damping ratios for the walls are virtually identical. For drift ratios between 50% and 100% of those associated with peak strength, for which elastic dynamic analysis might be employed, the equivalent viscous damping ratios of flexure-critical SC walls varies from 7.5% to 10%. At drift ratios greater than those associated with peak strength, SC1 had the greatest viscous damping because its strength deteriorated more slowly than the other walls.

### Displacement Components

Figure 7 describes the three contributions to the lateral displacement at the top of the SC walls, namely, flexural displacement,  $\Delta_f$ , shear displacement,  $\Delta_s$ , and lateral displacement due to base rotation,  $\Delta_r$ . The illustration is a section cut at a faceplate and not an elevation. The out-of-plane (vertical) deformation of the baseplate attached to the steel faceplates allowed rotation at the base of the wall. The displacement at top of the wall due to the base rotation,  $\Delta_r$ , was calculated using the vertical displacements measured by the first row of LEDs (see Figure 7):

$$\Delta_r = \theta_b H \quad (2)$$

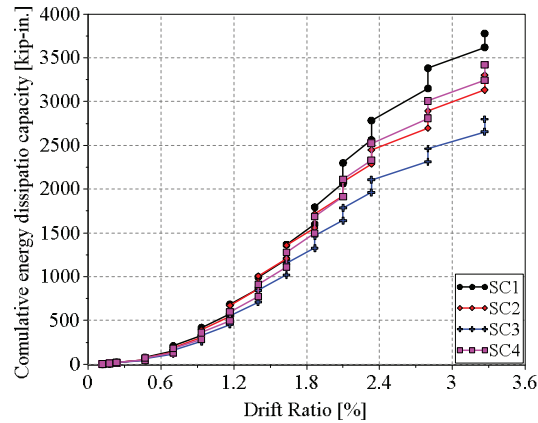


Figure 5. Cumulative energy dissipation in the SC walls

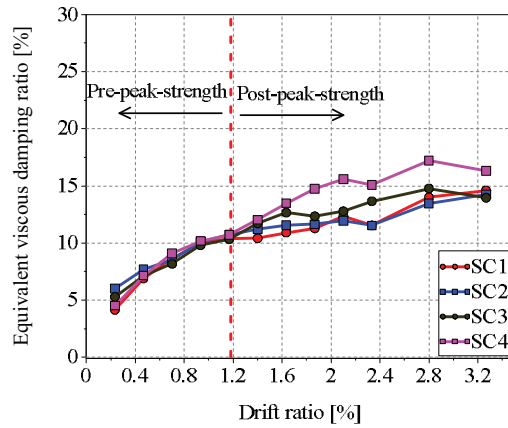


Figure 6. Equivalent viscous damping ratio

The base rotation was calculated as the average of the angles between the horizontal axis and the lines connecting LEDs 4 to 9, 5 to 8, and 6 to 7. The grid of Krypton LEDs generated horizontal strips across the surface of a faceplate as presented in Figure 8. The shear displacement in each strip was calculated as the product of the average shear strain, calculated using displacements measured by the LEDs, in the square panels comprising the strip, and the height of the strip,  $h_s$ . The shear component of the total lateral displacement at top of the wall was approximated as the product of the sum of the shear displacements of the horizontal strips (strips 1 to 9 in Figure 8) and the ratio of  $H_w/H_s$ , where the heights  $H_w$  and  $H_s$  are identified in Figure 8. The flexural component of the total lateral displacement at top of the wall was calculated as the difference between the total lateral displacement and the sum of the shear displacement and the lateral displacement due to the base rotation.

The contributions to the total lateral displacement of SC1 through SC4 are presented in Figure 9. As the lateral displacement increased, the percent contribution of the base rotation to the total displacement increased and the contributions of the shear and flexure displacements decreased. The contributions of the shear and flexural displacements to the total displacement varied from 35% at a drift ratio of 0.1% to 10% at a drift ratio of 2.5%. Figure 9 indicates that the displacement due to the base rotation governed the total lateral displacement at top of the SC walls. These results indicate that the baseplate connection between the SC wall and the foundation block was the major source of the flexibility in these walls and it needs to be carefully considered in the analysis, design, and detailing of SC walls with bolted baseplate to RC foundation connections.

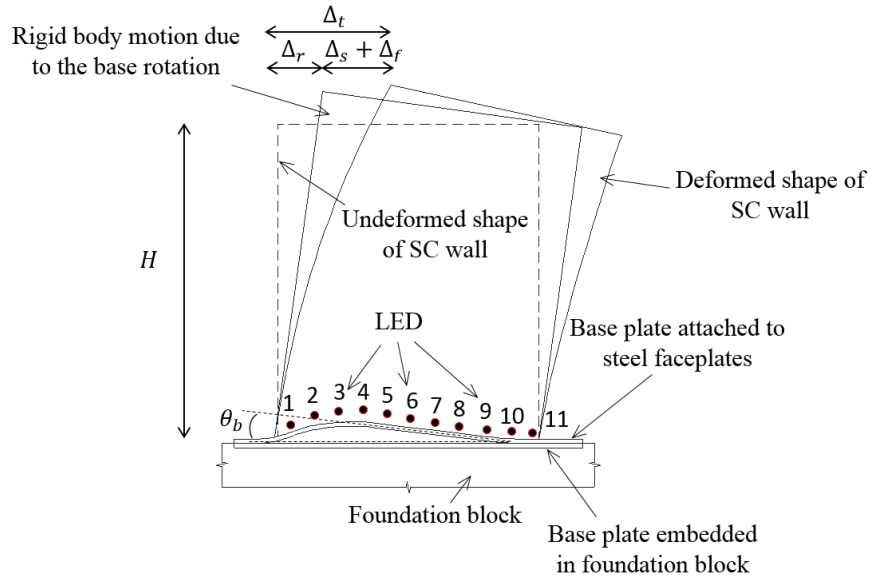


Figure 7. Components of the lateral displacement at top of the wall

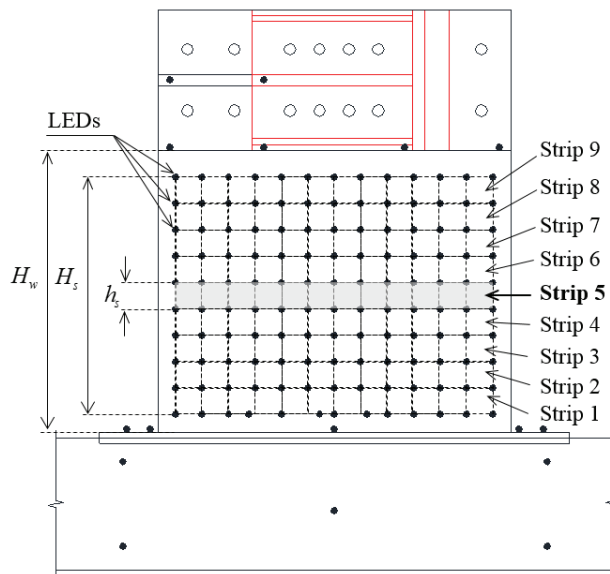


Figure 8. Definition of the horizontal strips for the shear displacement calculation

## CONCLUSIONS

This study investigated the cyclic inelastic behavior of SC walls. Four large-scale SC walls, SC1 through SC4, with an aspect ratio of 1.0 were tested at the University at Buffalo. The specimens were anchored to a concrete basemat with a pre-tensioned bolted connection that was designed to be stronger than the walls. The design parameters considered in the experimental investigation were wall thickness (9 in. and 12 in.), reinforcement ratio (3.1% and 4.2%), and faceplate slenderness ratio (21, 24, and 32).

The key conclusions of the study reported herein are:

1. Damage to flexure-critical SC walls in pre-peak-strength region included concrete cracking at toes of the wall at drift ratios less than 0.15% and steel faceplate buckling at 0.5% drift ratio. Concrete crushing

occurred at peak load. Tearing of the steel faceplates was first observed in post-peak-strength region of response.

2. To improve seismic response, tie rods instead of shear studs are recommended near the base and along the free edges of an SC wall, where the faceplates are likely to buckle and high tensile forces are imposed on the connectors.
3. Pinching in the hysteretic response of the SC walls is attributed to the cracking and crushing of the infill concrete, tearing of the steel faceplates, and flexibility at the base of the wall due to the baseplate connection.
4. The equivalent viscous damping for flexure-critical SC walls can be assumed to be 5% at displacements less than that at peak strength and 10% for greater displacements.
5. The displacement due to the base rotation governed the total lateral displacement for the SC walls with a bolted baseplate to RC foundation connection, indicating the importance of addressing foundation flexibility in design and analysis of SC walls.

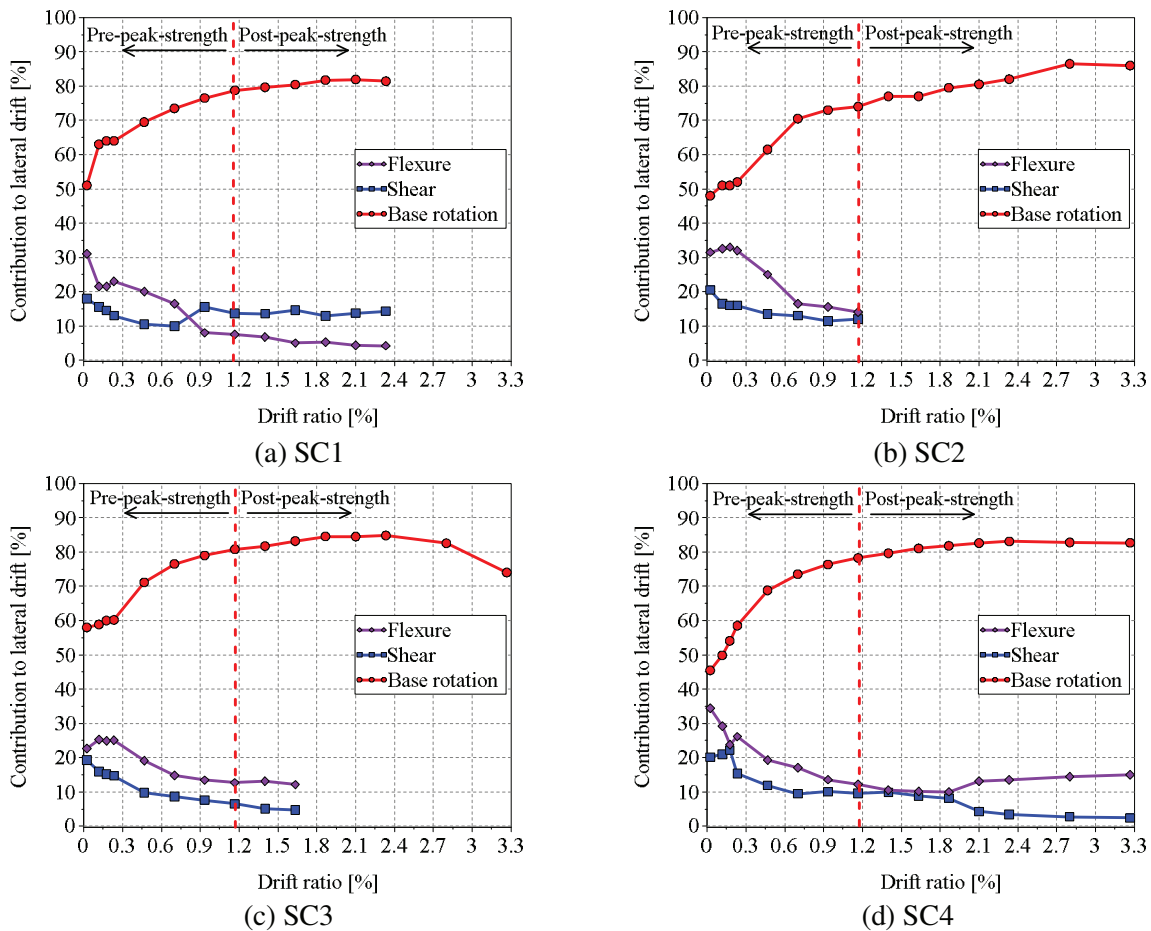


Figure 9. Contribution of the lateral displacement components to the total displacement

## ACKNOWLEDGEMENTS

This project was supported in part by the US National Science Foundation under Grant No. CMMI-0829978. This support is gratefully acknowledged. We thank the following individuals/group for their contributions to the research project: laboratory technicians and staff at University at Buffalo and Purdue University, Mr. Nam H. Nguyen, Mr. Efe Kurt, and LPCiminelli Inc.

## REFERENCES

- [1] Bowerman, H., Coyle, N., and Chapman, J. C. (2002). "An innovative steel/concrete construction system." *The Structural Engineer*, 80(20), 33-38.
- [2] Chopra, A. K. (2012). "Dynamics of structures: theory and applications to earthquake engineering (4th Edition)" Prentice Hall, Englewood Cliffs, New Jersey.
- [3] Epackachi, S. (2014). "Experimental, numerical, and analytical studies on the seismic response of steel-plate concrete (SC) composite shear walls" PhD dissertation, University at Buffalo, Buffalo, NY.
- [4] Epackachi, S., Nguyen, N. H., Kurt, E. G., Pitman, M., Weinreber, S., Whittaker, A. S., and Varma, A. H. (2014). "Steel-plate composite shear wall - Specimens SC1, SC2, SC3, and SC4." Network for Earthquake Engineering Simulation, DOIs:10.4231/D3BG2H97F (SC1)-10.4231/D36T0GW54 (SC2)-10.4231/D3319S315 (SC3)-10.4231/D3Z892F6J (SC4)
- [5] Epackachi, S., Nguyen, N. H., Kurt, E. G., Whittaker, A. S., and Varma, A. H. (2014). "In-plane seismic behavior of rectangular steel-plate composite wall piers." *Journal of Structural Engineering*.
- [6] Epackachi, S., Nguyen, N. H., Kurt, E. G., Whittaker, A. S., and Varma, A. H. "Numerical and experimental investigation of the in-plane behavior of rectangular steel-plate composite walls." *Proc., Structures Congress 2014*, American Society of Civil Engineers, 2478-2487.
- [7] Epackachi, S., Whittaker, A. S., and Huang, Y. N. (2014). "Analytical modeling of rectangular sc wall panels." *Journal of Construction Steel Research*, 105, 49-59.
- [8] Fukumoto, T., Kato, B., and Sato, K. (1987). "Concrete filled steel bearing walls." *IABSE report*, Zurich.
- [9] Tomlinson, M., Chapman, M., and Wright, H. D. (1989). "Shell composite construction for shallow draft immersed tube tunnels." *ICE international conference on immersed tube tunnels techniques*, Manchester, UK.
- [10] Varma, A. H., Malushte, S., Sener, K., and Lai, Z. (2013). "Steel-plate composite (SC) walls for safety related nuclear facilities: design for in-plane force and out-of-plane moments." *Nuclear Engineering and Design*, 269(1).
- [11] Varma, A. H., Zhang, K., Chi, H., Booth, P. N., and Baker, T. (2011). "In-plane shear behavior of SC composite walls: theory vs. experiment." *21th International Conference on Structural Mechanics in Reactor Technology (SMiRT21)*, International Association for Structural Mechanics in Reactor Technology (IASMiRT), New Delhi, India.
- [12] Wright, H. D. (1995). "The behavior of composite walling under construction and service loading." *Journal of Constructional Steel Research*, 35(3), 257-273.
- [13] Wright, H. D., Evans, H. R., and Gallocher, S. C. (1992). "Composite walling." *Engineering Foundation Conference*, Missouri, USA.
- [14] Wright, H. D., Hossain, K. M. A., and Gallocher, S. C. (1994). "Composite walls as shear elements in tall structures." *ASCE Structures Congress XII*, Atlanta, GA, USA, 140-145.
- [15] Zhang, K., Varma, A. H., Malushte, S. R., and Gallocher, S. (2014). "Effect of shear connectors on local buckling and composite action in steel concrete composite walls." *Nuclear Engineering and Design*, 269, 231-239.